Available online at www.sciencedirect.com
ScienceDirect
Journal of Catalysis 243 (2006) 221–228
JOURNAL OF CATALYSIS
www.elsevier.com/locate/jcat

Effect of carbon chain length on esterification of carboxylic acids with methanol using acid catalysis

Yijun Liu, Edgar Lotero, James G. Goodwin Jr. *

Department of Chemical and Biomolecular Engineering, Clemson University, Clemson, SC 29634, USA

Received 1 May 2006; revised 12 June 2006; accepted 12 July 2006

Available online 6 September 2006

Abstract

This paper reports on an investigation into the impact of carboxylic acid chain length on the kinetics of liquid-phase acid-catalyzed esterification. Using sulfuric acid and a commercial Nafion/silica composite solid acid catalyst (SAC-13), initial kinetics were measured for the reactions of a series of linear chain carboxylic acids (acetic, propionic, butyric, hexanoic, and caprylic acid) with methanol at 60 °C. It was found that reaction rate decreased as the number of carbons in the linear alkyl chain increased for both H_2SO_4 and SAC-13. This trend is discussed in terms of the polar and steric effects of the alpha-substituent to the carboxylic group and evaluated by a Taft-type correlation. Using a mechanistically based kinetic model, the reaction kinetic parameters of SAC-13 catalysis were determined and compared for different carboxylic acids. Moreover, important parameters, such as water deactivation, catalyst reusability, and regeneration, were also affected by the size of the carboxylic acid used. SAC-13 underwent significantly more activity loss with subsequent reaction cycles as the size of the alkyl tail on the carboxylic acid increased. Characterization of the catalyst after reaction suggested that the deactivation of SAC-13 is likely caused by the entrapment of bulky reaction intermediates in or on Nafion polymeric nanodomains blocking catalytic acid sites.

Keywords: Carboxylic acid; Esterification; Acid catalysis; Carbon chain length effect; Deactivation; Nafion/silica; Sulfuric acid

1. Introduction

Esterification of carboxylic acids with alcohols represents a well-known category of liquid-phase reactions of considerable industrial interest due to the enormous practical importance of organic ester products [1–3]. Recently, the acid-catalyzed esterification of long-alkyl chain fatty acids has spurred a great deal of interest, because long-chain fatty acid alkyl esters can be used as a biofuel. The reaction is especially important in the synthesis of biodiesel from low-cost feedstocks containing large amounts of free fatty acids (FFAs) [4–6]. Such FFAs must first undergo acid-catalyzed esterification before transesterification of the larger triglycerides is carried out using a base catalyst (usually NaOH) [7,8].

Currently, the esterification of fatty acids with alcohols is achieved commercially using liquid acid catalysts, such as sulfuric acid, hydrochloric acid, and para-toluenesulfonic acid (*p*-TsOH). The scientific literature contains some reports on the use of heterogeneous acid catalysts for esterification. The most popular solid acids used to produce esters have been ion-exchange organic resins, such as Amberlyst-15 [9], zeolites [10], and silica-supported heteropoly acids (HPA/silica) [11,12]. Nevertheless, they have been shown to exhibit limitations in applicability for catalyzing esterification due to low thermal stability (Amberlyst-15, <140 °C), mass transfer resistance (zeolites) [13,14], or loss of active acid sites in the presence of a polar medium (HPA/silica) [12,15].

SAC-13, a Nafion/silica nanocomposite [16], has been marketed as a new generation of supported resin catalyst. It has higher acid strength than conventional strong solid acids like H-ZSM-5, SO_4^{2-}/ZrO_2, and SiO_2/Al_2O_3 [17], higher thermodynamic stability than the polystyrene-based resins (Amberlyst, Dowex), and highly accessible acid sites due to the porous silica matrix [18]. The porous structure of the silica support with adjustable pore openings at the nanometer scale [16] diminish the likelihood of mass diffusion limitations, making it favor-

* Corresponding author. Fax: +1 864 656 0784.
E-mail address: james.goodwin@ces.clemson.edu (J.G. Goodwin Jr.).

0021-9517/$ – see front matter
doi:10.1016/j.jcat.2006.07.013

able for bulky reactants. This eco-friendly solid acid could have great potential for esterification reactions of FFAs as found in lipid feedstocks used for biodiesel production.

Although low-molecular-weight carboxylic acids have been widely used to address fundamental issues of esterification due to their simplicity, availability, and ease of reaction analysis, in general, good kinetic information on acid-catalyzed FFA esterification is quite limited. Certainly, having correlations between chemical structure and chemical reactivity provide insight into differences in chemical behavior between low-molecular-weight carboxylic acids and their larger and bulkier counterparts, FFAs. Dating back to the 1950s, researchers have conceptualized and quantified some of the possible effects of substituents on the chemical reactivity of alkyl esters in hydrolysis reactions [19]. The Hammett equation in aromatic systems and the Taft equation in aliphatic systems were the first proposed models that attempted to quantify polar, resonance, and steric effects of substituents in chemical reactivity [19]. These models were followed by extensive efforts to improve [20], modify [21], and expand them to other reactions [22]. Although most studies have been limited to the use of homogeneous catalysts, the qualitative conception and quantitative correlations reported in them provide a rational basis for understanding probable structural effects of large carboxylic acids on the activity of heterogeneous catalysts [23,24].

In contrast to the extensive studies done on the structural effect of carboxylic acids on homogeneous catalyzed esterification, this topic has been hardly explored for heterogeneous catalysis. Only a couple of studies related to this topic can be found in the literature: Lilja et al. [24], using ion-exchanged resins, and Mochida et al. [23], using sodium-poisoned silica–alumina. But these two studies used only straight alkyl chain carboxylic acids, no larger than butyric acid, and made no direct kinetic comparisons between homogeneous and heterogeneous catalysis. Thus, in an effort to develop a better understanding of the relationship between the existing fundamental knowledge obtained for esterification using low-molecular-weight carboxylic acids and the behavior of fatty acids in heterogeneous acid-catalyzed esterification, a set of linear-chain carboxylic acids (acetic acid [HAc], propionic acid [HPr], butyric acid [HBu], hexanoic acid [HHx], caprylic acid [HCp]) were used in this work. H_2SO_4 was used as a reference liquid catalyst to carry out reaction studies under identical experimental conditions as those for the solid acid, SAC-13, allowing for a more precise rationalization of the results obtained with the heterogeneous catalyst SAC-13. In addition, for the solid catalyst, the impact of increasing the carboxylic carbon chain length acid on catalyst deactivation, reusability, and regeneration was investigated.

2. Experimental

Reagents including methanol (99.9 wt%, Acros Organics), HAc (99.7 wt%, Aldrich), HPr (99.0 wt%, Aldrich), HBu (99.0 wt%, Aldrich), HHx (99.5 wt%, Aldrich), and HCp (99.0 wt%, MP Biomedicals) were used without further purification. Concentrated sulfuric acid was purchased from Fisher Scientific, and SAC-13 was obtained from Aldrich.

The sulfur content of SAC-13 was determined by elemental analysis using ICP (Galbraith Laboratory, Knoxville, TN). BET surface area, pore diameter, and BJH cumulative pore volume were obtained using N_2 adsorption at −196 °C in a Micromeritics ASAP 2020. Before N_2 adsorption, the catalyst samples were outgassed for 3 h at 120 °C. IR spectra were recorded using a Nicolet Avatar 360 FTIR spectrometer equipped with a nitrogen-purged chamber and DRIFT attachment. Thermogravimetric analysis (TGA) was done using a Pyris 1 analyzer (Perkin–Elmer) to characterize the used catalysts. Under a nitrogen flow of 20 ml/min, the temperature was first stabilized at 25 °C for 30 min and then ramped to 700 °C at 10 °C/min.

Reactions were carried out in an isothermal batch reactor (Parr 4590) as described previously [25,26]. Typically, a reaction temperature of 60 °C was used. Catalyst loadings of 1.09 and 0.022 g in the reaction mixture of 45 ml were used for SAC-13 and H_2SO_4 (5 mM), respectively. The absence of mass transfer limitations and catalyst swelling for SAC-13 was experimentally determined as described previously [26], thus ensuring the measurement of intrinsic reaction kinetics. THF was used as a solvent to fix the concentrations of carboxylic acids at 3 M and methanol at 6 M and also to ensure complete miscibility of all carboxylic acids/methanol reagent mixtures investigated.

At particular times of reaction, 30–60 μl reaction mixture samples were obtained using a microscale syringe. Samples from the reaction mixture were immediately chilled and diluted in cold 2-propanol to minimize any residual reaction. A Hewlett–Packard 6890 gas chromatograph equipped with an FID detector and a split/splitless inlet was used for sample analysis. A DB-1 column (0.32 mm × 30 m × 0.53 μm) was used for analysis of the HAc and HPr reactions using ethanol as the internal standard. A CP-SIL 5CB column (0.25 mm × 10 m × 0.12 μm) was used for the HBu, HHx, and HCp reaction analysis with methyl laurate as the internal standard.

Autocatalysis was negligible compared with SAC-13 or H_2SO_4 catalysis under the experimental conditions used; thus it did not have to be accounted for in the rate determinations. In addition, kinetic measurements focused particularly on the initial period of reaction (<10%) to minimize the impact of reverse hydrolysis. The determination of initial reaction rate used the same methodology as described previously [26].

3. Results and discussion

3.1. Reactivity of carboxylic acids

Figs. 1a and 1b show the reactivity differences of the carboxylic acids for esterification with methanol at 60 °C catalyzed by sulfuric acid and SAC-13, respectively. On a per weight basis, the homogeneous acid catalyst was much more active than the heterogeneous catalyst, due to the lower acid site concentration of the latter. A 10% carboxylic acid conversion was achieved within 3–8 min using 5 mM (0.022 g/45 ml) H_2SO_4 at 60 °C with 2× stoichiometric methanol. However, it took 20–

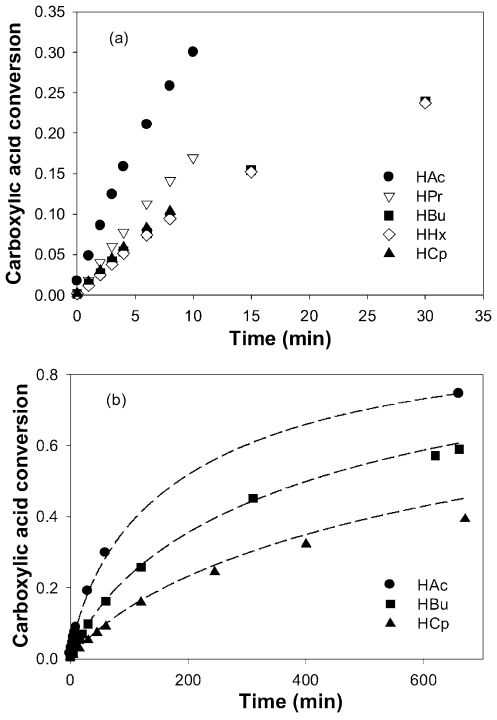

Fig. 1. Reactivity of different carboxylic acids in esterification catalyzed by (a) H_2SO_4 (5 mM) and (b) SAC-13 (1.09 g/45 ml) at 60 °C ($C_{A,0} = 3$ M, $C_{M,0} = 6$ M, symbols represent the experimental data; dotted lines represent the model prediction).

Table 1
TOF values calculated for sulfuric acid and SAC-13 catalyzed esterification of different carboxylic acids with methanol at 60 °C ($C_{A,0} = 3$ M, $C_{M,0} = 6$ M)

	HAc	HPr	HBu	HHx	HCp
			TOF (min^{-1})[a]		
H_2SO_4[b]	22.76	12.12	7.42	7.98	8.46
SAC-13[c]	7.28	4.75	2.87	2.22	1.47
			v[31]		
$\log r = \psi v + h$	0.52	0.56	0.68	0.68	0.73

[a] Experimental error ±6%.
[b] 1 mol H^+/1 mol H_2SO_4 is assumed.
[c] 0.131 mmol H^+/g was used [26].

60 min for esterification to reach the same level of conversion when using 1.09 g SAC-13 as a catalyst. Furthermore, HAc esterification using SAC-13 required several hundred minutes to approach equilibrium conversion; esterification of the bulkier HCp took even longer to do the same. Table 1 summarizes activity differences of the two catalysts in esterification at 60 °C using turnover frequencies (TOFs) based on the assumption of 1 M H^+/1 M H_2SO_4 and 0.13 mmol of acid sites/1 g SAC-13 [26]. Thus, on a per site basis, the catalytic activities of H_2SO_4 and SAC-13 were much more comparable, with H_2SO_4 being only 2–5 times more active than SAC-13 for the set of carboxylic acids investigated.

The decreasing trend in carboxylic acid reactivity with increasing alkyl chain length using acid catalysis is evident in both Table 1 and Fig. 1. The reactivity loss per additional –CH_2– moiety was greatest for the small carboxylic acids from HAc to HBu for both liquid and solid catalysts. However, in the case of H_2SO_4, the effect of chain length on reactivity was indiscernible for carboxylic acids larger than HBu. The observed reactivity trend for carboxylic acids can be conceptualized using the homogeneous catalysis mechanism model for esterification [27]. Initially, two components contribute to the diminished carboxylic acid reactivity with size: an inductive effect and a steric effect [19]. The inductive effect results from the increase in electron-releasing ability of the acid with lengthening alkyl chain. Although the inductive effect facilitates the protonation of the carbonyl oxygen, it also lowers the electrophilicity of the carbonyl carbon, resulting in a more energy-hindered rate-limiting nucleophilic attack by the alcohol.

The steric component affecting carboxylic acid reactivity is perhaps the decisive factor for acid-catalyzed esterification [19,21,28]. Steric hindrance increases with molecular size, inducing electronic repulsion between nonbonded atoms of reacting molecules. This repulsive hindrance lowers electron density in the intermolecular region and disturbs bonding interactions [28]. Thus, as the alkyl chain in the carboxylic acid increases in size, its steric effect increases as well. However, steric constraints are governed not only by the size of molecules, but also by their preferential conformations [29,30]. This gives rise to the so-called "conformational leveling" effect [30]. Thus, the reactivity plateau exhibited by HBu, HHx, and HCp for H_2SO_4 catalysis (Table 1 and Fig. 1) may be understood based on this established principle. More specifically, in homogeneous catalysis, large carboxylic acid molecules may assume conformations that minimize contributions to steric hindrance. The probable conformations for the reaction intermediates must be in a dynamic equilibrium, likely favoring those allowing the reaction.

In contrast, any conformational leveling effect in heterogeneous catalysis seems to be limited, as suggested by the reactivity gap observed for reactions using HBu, HHx, and HCp (Table 1). This is likely due to the reduced conformational freedom of adsorbed alkyl groups on the SAC-13 catalyst. Additional interactions of the carboxylic acid, while bonded to the acid site, with polymer moieties of the Nafion nanodomains and/or surrounding silanol groups also may play a role here. As a result, it is more difficult for methanol molecules to reach the protonated carboxylic group when there is a large alkyl chain blocking access.

As the evidence suggests, steric considerations are less important for acid sites free in solution (homogeneous catalysis) than for acid sites fixed on a surface. Likewise, conformational constraints underwent by intermediates during heterogeneous catalysis should also account for the lower site activity of SAC-13 compared with H_2SO_4 (Table 1). Nonetheless, conformational restrictions should weaken at high reaction temperatures. For instance, at 250 °C, Mochida et al. [23] observed only small steric effects in the esterification of different carboxylic acids with a wide range of structures using sodium-doped silica–alumina. At high temperature, reaction intermediates on the solid surface have a shorter residence time due to fast adsorption/desorption dynamic equilibrium. Thus, conformational restrictions are compensated for in part by the rapid exchange of absorbed and in-solution species.

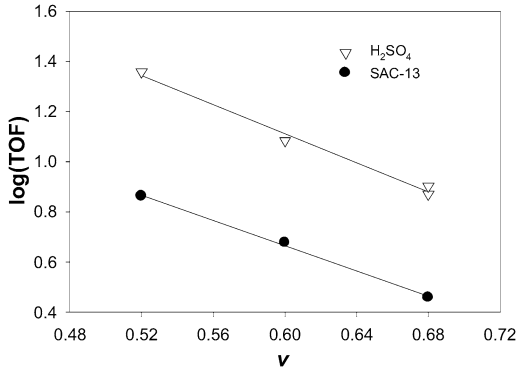

Fig. 2. Charton correlation for H_2SO_4 (HAc, HPr, HBu, and HHx) and SAC-13 (HAc, HPr, and HBu) catalysis.

On the basis of linear free-energy relationships (LFERs), Taft quantitatively evaluated the steric effect caused by substituents in aliphatic systems using the correlation $\log(r/r_0) = \delta E_S$ [19]. Here r/r_0 represents the reactivity ratio of a carboxylic acid having a given substituent versus one with $–CH_3$ (acetic acid), which is the reference group; E_S characterizes the steric hindrance associated with a substituent relative to that of $–CH_3$; and δ serves as a measure of the susceptibility of a particular reaction series to the steric effects of substituents. Charton [21] further improved the Taft correlation by replacing the E_S constant with the van der Waals radii v associated with a given substituent and proposed the equation $\log r = \psi v + h$, where ψ and h are constants.

The v values for alkyl chains have been determined using homogeneously catalyzed esterification [31]. Using the results and the Charton equation to correlate the probable steric hindrance from low-molecular-weight carboxylic acids on H_2SO_4 and SAC-13 resulted in linear plots with similar dependences on v (Fig. 2). This suggests that steric effects indeed dominate catalyst activity in acid-catalyzed esterification of small carboxylic acids (HAc to HBu) for both H_2SO_4 and SAC-13 and that the two catalysts share similar steric-reactivity responses for these small reactants.

3.2. Kinetic parameters for the esterification of carboxylic acids in SAC-13 catalysis

In a recent study [26], we showed that SAC-13-catalyzed esterification involves single-site catalysis similar to what occurs using a homogeneous acid catalyst. The following kinetic model, derived using a hypothesized mechanism with strong parallels to that proposed for homogeneous acid-catalyzed esterification, was validated by its excellent representation of experimental data for acetic acid esterification on SAC-13 [26]:

$$\frac{dC_A}{dt} = \frac{kC_C C_{A,0}}{1 + (K_M C_M + K_A C_A + K_W C_W)}\left(C_M C_A - \frac{C_W C_E}{K_e}\right), \quad (1)$$

Here k is the lumped reaction constant, C denotes concentrations, and K represents adsorption equilibrium constants with the exception of K_e, which represents the equilibrium constant for esterification. The subscript M stands for methanol; A, for carboxylic acid; W, for water; and E, for the ester. From a mechanistic standpoint, Eq. (1) represents a rate-controlling surface reaction between adsorbed carboxylic acid and free methanol in the bulk phase. The terms for methanol and water in the denominator of Eq. (1) correspond to their competitive site occupation with carboxylic acid owing to their intrinsic larger proton affinities.

For a molar ratio of $C_{M,0}/C_{A,0} = n$ and an initial water addition of $C_{W,0}/C_{A,0} = u$, Eq. (1) expressed in terms of carboxylic acid conversion (x_A) becomes

$$\frac{dx_A}{dt} = \frac{kC_C C_{A,0}}{1 + C_{A,0}[K_M(n - x_A) + K_A(1 - x_A) + K_W(x_A + u)]} \times \left[(n - x_A)(1 - x_A) - \frac{(x_A + u)x_A}{K_e}\right]. \quad (2)$$

Using the same methodology outlined in previous work [26], we determined the kinetic and equilibrium adsorption parameters for the esterification of HBu and HCp. These are summarized in Table 2 together with those for HAc esterification. A quick look at these constants shows that catalyst surface coverage of methanol and water decreases as the alkyl chain of the reacting carboxylic acid increases. In particular, the adsorption of methanol on surface acid sites is noticeably affected by HCp. The opposite trend might have been expected given the polar and hydrophilic nature of methanol, which could have been expected to preferably bond to the Nafion domains on SAC-13 [18] while hindering the contact of other hydrophobic reactants with the catalyst surface. The decreased methanol adsorption on the catalyst, however, may suggest a longer residence time for the carboxylic acids on the Brønsted sites of SAC-13 with increasing alkyl chain length. It is likely, then, that adsorbed HCp is able to modify the catalyst surface affecting alcohol adsorption.

Using the kinetic and adsorption equilibrium parameters listed in Table 2 and numerical integration (Runga–Kutta), carboxylic acid conversion at a given time can be predicted from Eq. (2). The dotted lines in Fig. 1b depict calculations of esterification progress from Eq. (2). Thus, Eq. (2) can satisfactorily represent the evolution of esterification for small acids with methanol on SAC-13. However, the model somewhat overestimates the conversion profile for the bulkier HCp. So, given that Eq. (2) was derived from initial kinetics, some unaccounted-for deactivating factors may be coming into play as the reaction

Table 2
Adsorption equilibrium constants for methanol, carboxylic acids and water, reaction constant k for SAC-13 and reaction equilibrium constants for different carboxylic acid esterifications at 60 °C

Reactant	HAc	HBu	HCp
k[a] (L^2/g catal mol min) × 10^4	1.50	0.50	0.20
K_e[b]	6.20	5.70	5.50
K_M[a](L/mol)	0.16	0.11	0.02
K_A[a](L/mol)	0.13	0.07	0.10
K_W[a](L/mol)	3.11	2.12	1.78
K_W/K_A	24	30	18

[a] Experimental error ±5%.
[b] Experimental error ±6%.

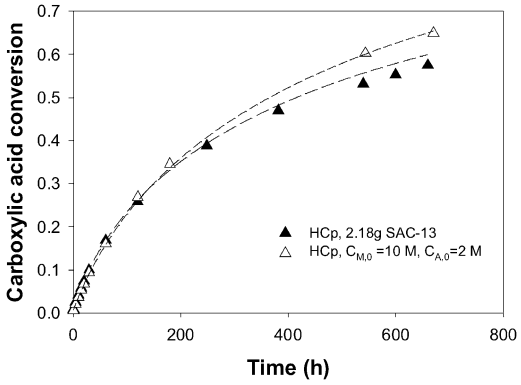

Fig. 3. Comparison of experimental data with values predicted by Eq. (1) for esterification of HCp with methanol under different reaction conditions (symbols represent the experimental data; dotted lines represent the model prediction).

progresses that become more important as the reacting acid increases in size. For instance, when the derived mathematical model is applied to the HCp esterification using twice the amount of catalyst ($C_C = 2.18$ g/45 ml) or a higher molar ratio of methanol to HCP ($n = C_{M,0}/C_{A,0} = 5$), the quantitative prediction precision of Eq. (2) is greatly improved, as shown in Fig. 3. However, the good agreement between predicted and experimental data suggests identical reaction mechanistic routes [26] in all cases under SAC-13 catalysis.

3.3. Catalyst deactivation in esterification of carboxylic acids

3.3.1. Water deactivation

The effect of water on reaction is important in esterification because H_2O is continuously produced as a byproduct. Certainly, the presence of water promotes the reverse reaction; however, the effect of water on catalyst activity is even more critical, as has been previously shown by us for H_2SO_4-catalyzed [25] and SAC-13-catalyzed [26] esterification of acetic acid.

The hydrophobicity of the reacting carboxylic acid increases with increasing carbon chain length. Here, using different carboxylic acids, the impact of reactant hydrophobicity on the water inhibition effect was compared. The parallel lines shown in the logarithmic plots of initial reaction rate versus water concentration (Fig. 4) clearly indicate that the deactivating behavior of water is not a function of the hydrophobicity of the reacting acids in a wide range of water concentration (0.45–3 M) for both heterogeneous and homogeneous acid catalysts. As can be seen, only the most hydrophobic reactants show some protection over acid sites in the low water concentration range (<0.45 M) given the very high proton affinity of water [25]. Despite the somewhat decreased adsorption equilibrium constant of water on acid sites in HCp esterification (Table 2), the site affinity of water remained about 20 times greater than that of the carboxylic acids, as indicated by the K_W/K_A ratio given in Table 2. In this respect, the information obtained from this fundamental study using low-molecular-weight model compounds helps us better understand the esterification of FFAs contained in lipid feedstocks, such as vegetable oils and animal fats.

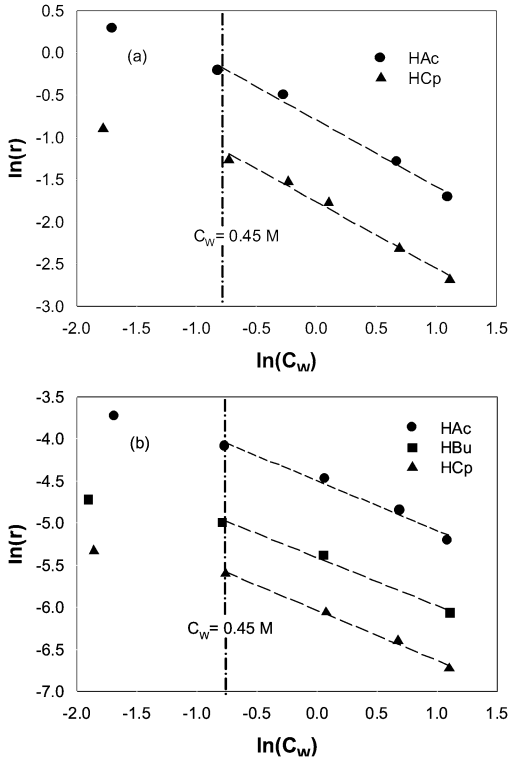

Fig. 4. The impact of carboxylic acid hydrophobicity on the water inhibition effect using (a) SAC-13 and (b) H_2SO_4.

3.3.2. Catalyst reusability and regeneration

The reusability of solid catalysts is one of their main advantages over liquid homogeneous catalysts. To evaluate this characteristic for the SAC-13 catalyst, the esterification reactions of HAc, Hbu, and HCp at 60 °C were investigated by running consecutive reaction cycles using the same reaction conditions as described earlier. Each reaction cycle took 11 h for HAc and HBu esterification and 24 h for HCp esterification, so that the latter could reach a similar conversion level (60–75%) at the end of the first reaction cycle. After each cycle, reaction mixtures were decanted, the catalyst was recovered, and a new reaction cycle was started with fresh reactants. The relative initial catalytic activity for each cycle is plotted in Fig. 5. Continuous activity loss of SAC-13 with each reaction cycle was observed for all carboxylic acids. Catalyst reusability was highest for HAc esterification, with SAC-13 retaining about 75% of its original activity after three 11-h cycles. SAC-13 underwent more significant deactivation with reactions involving larger carboxylic acids. For instance, after three 11-h cycles the catalyst retained only 65% of its initial activity in the first cycle for HBu and 50% of that for HCp.

Water produced from esterification can be expected to have inhibited SAC-13 catalytic activity. When catalysts were recovered from reaction mixtures and reused with fresh reactants with no catalyst treatment, the amount of water chemically and physically bonded to the catalyst surface from the previous cycle may have been an important factor in deactivation. However, the activity pattern shown in Fig. 5 cannot be explained totally by catalyst deactivation due to water clustering around the acid sites. Otherwise, reaction involving HAc esterification should

have shown the greatest deactivation, because this reaction had the highest conversion of carboxylic acid, 75% after the first reaction cycle of 11 h versus only 60% for HBu (11 h) and for HCp (24 h). Furthermore, according to Table 2, the acid sites of SAC-13 showed greater site coverage and a higher water adsorption equilibrium constant for HAc esterification than for esterification involving the larger carboxylic acids. Thus, it is unlikely that residual water on the catalyst surface after each reaction cycle was the most significant factor accounting for the observed differences in catalyst deactivation after multiple reaction cycles.

For reactions using HBu and HCp, an additional series of reaction cycles was carried out in an attempt to examine the possibility of catalyst regeneration by solvent washing. In these experiments, after the catalyst was recovered from each reaction cycle, it was washed extensively with THF and dried again under vacuum at 25 °C for 4 h before a new cycle was started with fresh reactants. The catalytic activity and conversion for each cycle are given in Table 3. THF washing was able to improve catalyst reusability for the reaction of HBu. Catalyst activity decreased by only 10% after two 11-h cycles, and this activity was maintained during the next two cycles. A different situation was observed for HCp, however; despite some improvement, THF washing was not able to maintain catalyst activity, and SAC-13 still exhibited a continuous activity loss after each reaction cycle. The initial activity lost after three reaction cycles was about 30%. For the cycling series of 11 h, the catalyst showed an almost identical deactivation profile to that observed in the cycling series of 24 h, suggesting that catalyst deactivation occurs early in the reaction cycles. In addition, increasing the temperature of vacuum pretreatment from 25 to 80 °C had little effect on catalyst reactivation (the fourth 24-h cycle of HCp; Table 3). Using alcohol washing of the spent catalyst, Alvaro et al. [32] reported excellent reusability for a "SAC-13 like" perfluoroalkylsulfonic acid-modified MCM-41 silica in the esterification of HCp with ethanol. The possible in situ washing ability of methanol could have been responsible for the better correlation of the derived mathematical model based on initial kinetics and experimental data when using a larger excess of methanol during reaction (Fig. 3); however, we found that methanol washing between cycles was no better for SAC-13 catalyst reusability than THF washing (Table 3).

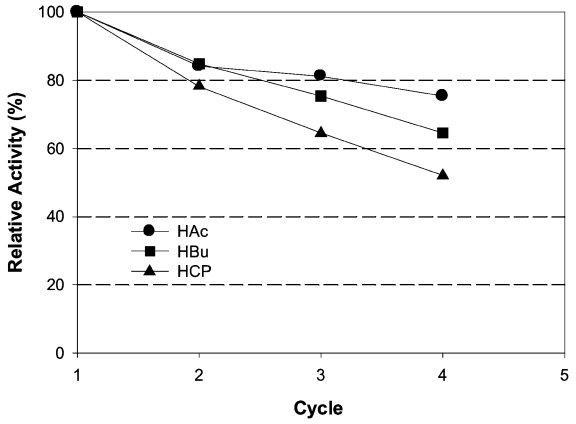

Fig. 5. SAC-13 deactivation following multiple reaction cycles of esterification of HAc, HBu, or HCp with methanol at 60 °C without any treatment. ($C_{A,0} = 3$ M, $C_{M,0} = 6$ M; catalyst loading = 1.09 g/45 ml; the cycling time was 11 h for HAc and HBu and 24 h for HCp.)

Sulfur leaching could have been a possible cause of the catalyst deactivation during multiple reaction cycles, as is known to occur for SO_4^{2-}/ZrO_2 [33,34]. Elemental analysis showed that the spent SAC-13 after four 11-h HCp esterification cycles maintained 96% of its original sulfur content, however.

Differences observed in catalyst reusability for reactions using different carboxylic acids suggest the entrapment of bulky reactants, intermediates, and products in the Nafion nanodomains as the most probable cause of the lost catalyst activity. Supporting this hypothesis, the spent catalyst after four HCp esterification cycles (using THF washing between) showed decreased BET surface area and pore volume but increased average pore diameter (Table 4), suggesting the blockage of micropores in the catalyst. In contrast, the spent catalyst after four reaction cycles using HBu had similar physical properties as fresh SAC-13, consistent with its better reusability.

FTIR was used to characterize the catalyst before and after reaction cycling. Fig. 6 shows IR spectra in the range 1200–

Table 3
SAC-13 deactivation following multiple reaction cycles of esterification of methanol and HBu/HCp at 60 °C with solvent washing and vacuum drying between cycles ($C_{A,0} = 3$ M, $C_{M,0} = 6$ M; catalyst loading = 1.09 g/45 ml)

Carboxylic acid	Cycling time (h)	Solvent for washing	Parameter	Reaction cycles			
				First	Second	Third	Fourth
HBu	11	THF	η[a]	100%	94.3%	90.4%	91.3%
			$x_{A,f}$[b]	0.59	0.57	0.54	0.54
HCp	24	THF	η[a]	100%	89%	77%	70%[c]
			$x_{A,f}$[b]	0.58	0.54	0.51	0.47
HCp	11	THF	η[a]	100%	88%	78%	68%
			$x_{A,f}$[b]	0.39	0.35	0.33	0.31
HCp	11	MeOH[d]	η[a]	100%	88%	77%	–
			$x_{A,f}$[b]	0.40	0.37	0.33	–

[a] $\eta = (r_{0,i}/r_{0,1}) \times 100\%$ is defined as the ratio of the initial reaction rate using the recycled catalyst to that using fresh catalyst.

[b] $x_{A,f} = (C_{A,0} - C_{A,f})/C_{A,0}$ is the conversion of carboxylic acid when each cycle ends.

[c] Catalyst was evacuated at 80 °C for 4 h after washing with THF at room temperature prior to the fourth cycle.

[d] Catalyst was washed in MeOH at 50 °C for 4 h followed by evacuation at 25 °C for 4 h.

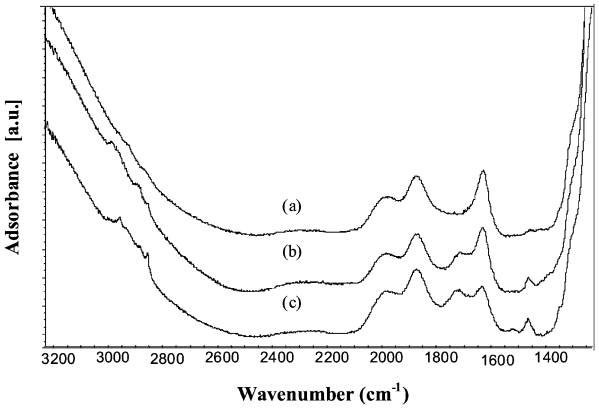

Fig. 6. IR spectra of SAC-13 samples: (a) fresh catalyst sample and used catalyst recovered from (b) HBu and (c) HCp esterification after four consecutive 11 h reaction cycles. (Spent catalyst samples were washed using THF and then evacuated at 25 °C after each cycle.)

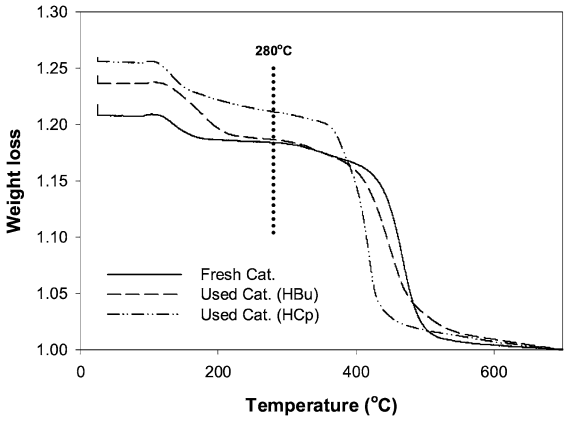

Fig. 7. Thermogravimetric analysis (TGA) of the fresh and the used catalyst samples recovered after HBu and HCp esterification for four consecutive 11 h reaction cycles. (Used catalyst samples were washed using THF and then evacuated at 25 °C after each cycle.)

Table 4
Physical properties of the fresh and used catalyst samples recovered after HBu and HCp esterification for four consecutive 11 h reaction cycles

Catalyst	S_{BET} (m^2/g)	Average pore diameter (Å)	Pore volume (cm^3/g)
Fresh SAC-13	233.6 ± 5.6	101.0 ± 2.3	0.59 ± 0.01
Spent SAC-13 (HBu)[a]	230.6 ± 4.8	103.7 ± 1.1	0.60 ± 0.01
Spent SAC-13 (HCp)[a]	179.0 ± 0.2	120.6 ± 0.3	0.55 ± 0.01

[a] Spent catalysts were washed using THF and then evacuated at 25 °C after each cycle.

3200 cm^{-1} for both fresh and spent catalyst samples. The peaks centered at 2900 and 1700 cm^{-1} that evolved for the used catalysts can be assigned to the stretching frequencies of $–CH_2–$/$–CH_3$ and C=O groups, respectively. Appearance of these signals together with the small band at 1460 cm^{-1}, which may be ascribed to the bending and/or scissoring vibration of C–H, provide evidence of the strong adsorption of carboxylic acids on the catalyst surface. Note that after multiple esterification cycles, the adsorption band at 1630 cm^{-1} due to the bending vibration of O–H bonds in water [35,36] weakens more on the HCp spent catalyst. This suggests a higher hydrophobic character for the surface of this material, conforming to the hypothesis of greater hydrocarbon accumulation on the catalyst surface when HCp is used.

Because FTIR is usually good only as a qualitative technique, TGA was carried out to make a further assessment of the hydrocarbon accumulation on the used SAC-13 catalysts. In the calculation, we assumed that the mass of silica matrix in the catalyst was unchanged by the reaction. Thus, the mass of the catalyst was normalized to the residual silica amounts at 700 °C. TGA profiles replotted in this way are shown in Fig. 7. As can be seen, spent catalysts recovered from the esterification of HCp show the greatest weight loss after 280 °C. It is at this temperature that the decomposition of the $–SO_3H$ moieties starts, marking the thermal degradation of Nafion nanodomains. Because at this temperature (280 °C) any physisorbed or reversibly chemisorbed compounds should have already desorbed, it is reasonable to ascribe the extra loss in mass (compared with the fresh catalyst sample) to strongly adsorbed organic species on the catalyst surface. Strong adsorption of larger organic compounds may occur through a combination of two pathways: (1) irreversible adsorption on acid Brønsted sites and (2) entanglement of long alkyl chains with the Nafion nanodomain polymeric chains in a "spaghetti-like" fashion.

Fig. 7 shows that the spent catalyst sample recovered from the esterification of HBu has a TGA profile after 280 °C similar to that of a fresh catalyst sample, suggesting little accumulation of strongly bonded hydrocarbon species on the SAC-13 catalyst, in accordance with the catalyst reusability pattern observed for this reaction (Table 3). Fig. 7 also indicates that the thermal stability of the Nafion perfluorinated polymeric backbone is affected by the presence of hydrocarbon species from reaction. For instance, for the catalyst after HCp reaction, rapid degradation starts at 375 °C, about 60 °C below the onset temperature for the degradation of a fresh catalyst sample. In contrast, the used catalyst from the HBu reaction is destabilized by only 20 °C compared with fresh catalyst. The shift in thermal stability of the used catalyst samples is probably caused by the faster decomposition of hydrocarbons (compared with fluorinated polymers), which facilitates the production of OH and/or carbon-based radicals. Radical species are known to act as reaction initiators in the degradation of the Nafion polymeric perfluorinated resin [37].

Consequently, TGA data support the hypothesis of greater accumulation of hydrocarbons from the HCp reaction on the used catalyst. This is in agreement with the concept of acid site blockage by the large carboxylic acids, hindering access to active sites and inhibiting catalyst activity. In addition, the larger the carboxylic acid, the more difficult its removal by solvent washing. However, it is possible that intensive catalyst washing with solvents [38] or techniques more apt to extract hydrocarbons, such as super critical fluid extraction [39], might in fact improve catalyst regeneration.

4. Conclusion

The impact of carboxylic acid carbon chain length on heterogeneous acid-catalyzed esterification using silica-supported

Nafion (SAC-13) was studied and compared with that using H_2SO_4. The reactivity of the carboxylic acids was controlled by steric factors as the alkyl chain grew linearly. The reactivity–structure response was similar for both liquid and solid acid catalysis for small carboxylic acids (HAc to HBu). For larger carboxylic acids (HBu to HCp), little if any additional impact of increasing chain length on reactivity for homogeneous catalysis was seen. A contrasting trend was observed for heterogeneous catalysis, however, with a continuous inhibitory effect on activity caused by increasing the chain length of the carboxylic acid. This difference was probably due to the restricted conformational freedom of molecules as they adsorbed on solid surfaces. Large carboxylic acids had little effect on water deactivation of Brønsted acid sites for both the liquid and solid catalysts, despite the increased hydrophobicity. Nevertheless, alkyl chain length had an important effect on SAC-13 reusability. Using THF washing, the Nafion/SiO_2 nanocomposite catalyst showed good reusability in the esterification of low-molecular-weight acids. However, the catalyst experienced continuous activity loss in consecutive reaction cycles using the larger HCp. Catalyst deactivation was probably due to accumulation of the carboxylic acid molecules/intermediates on or in the nanodomains of the Nafion resin. Such an accumulation may have been caused by the irreversible adsorption of carboxylic acids on Brønsted sites and/or their entanglement with the polymeric chains of the Nafion nanoparticles. Effective regeneration is needed to improve the applicability of SAC-13 in the esterification of large FFAs.

References

[1] G.D. Yadav, P.H. Mehta, Ind. Eng. Chem. Res. 33 (1994) 2198.
[2] M.R. Altiokka, A. Citak, Appl. Catal. A 239 (2003) 141.
[3] E. Ayturk, H. Hamamci, G. Karakas, Green Chem. 5 (2003) 460.
[4] E. Lotero, Y. Liu, D.E. Lopez, K. Suwannakarn, D.A. Bruce, J.G. Goodwin Jr., Ind. Eng. Chem. Res. 44 (2005) 5353.
[5] I.K. Mbaraka, D.R. Radu, V.S.Y. Lin, B.H. Shanks, J. Catal. 219 (2003) 329.
[6] I.K. Mbaraka, B.H. Shanks, J. Catal. 229 (2005) 365.
[7] F.R. Ma, M.A. Hanna, Bioresource Technol. 70 (1999) 1.
[8] M. Canakci, J. Van Gerpen, Trans. ASAE 44 (2001) 1429.
[9] G.D. Yadav, M.B. Thathagar, React. Funct. Polym. 52 (2002) 99.
[10] S.R. Kirumakki, N. Nagaraju, S. Narayanan, Appl. Catal. A 273 (2004) 1.
[11] W.L. Chu, X.G. Yang, X.K. Ye, Y. Wu, Appl. Catal. A 145 (1996) 125.
[12] J.H. Sepulveda, J.C. Yori, C.R. Vera, Appl. Catal. A 288 (2005) 18.
[13] B.R. Jermy, A. Pandurangan, Appl. Catal. A 288 (2005) 25.
[14] S.R. Kirumakki, N. Nagaraju, K.V.R. Chary, S. Narayanan, Appl. Catal. A 248 (2003) 161.
[15] Y. Izumi, K. Urabe, Chem. Lett. (1981) 663.
[16] M.A. Harmer, W.E. Farneth, Q. Sun, J. Am. Chem. Soc. 118 (1996) 7708.
[17] K. Okuyama, X. Chen, K. Takata, D. Odawara, T. Suzuki, S. Nakata, T. Okuhara, Appl. Catal. A 190 (2000) 253.
[18] Q. Sun, W.E. Farneth, M.A. Harmer, J. Catal. 164 (1996) 62.
[19] R.W. Taft, Steric Effects in Organic Chemistry, in: M.S. Newman (Ed.), Wiley, New York, 1956, pp. 556–675.
[20] J. McPhee, A. Panaye, J. Dubois, Tetrahedron 34 (1978) 3553.
[21] M. Charton, J. Am. Chem. Soc. 97 (1975) 1552.
[22] D.F. DeTar, J. Org. Chem. 45 (1980) 5174.
[23] I. Mochida, Y. Anju, A. Kato, T. Seiyama, Bull. Chem. Soc. Jpn. 44 (1971) 2326.
[24] J. Lilja, D.Y. Murzin, T. Salmi, J. Aumo, P.M. Arvela, M. Sundell, J. Mol. Catal. A 182 (2002) 555.
[25] Y. Liu, E. Lotero, J.G. Goodwin Jr., J. Mol. Catal. A 245 (2005) 132.
[26] Y. Liu, E. Lotero, J.G. Goodwin Jr., J. Catal. 242 (2006) 187.
[27] R. Ronnback, T. Salmi, A. Vuori, H. Haario, J. Lehtonen, A. Sundqvist, E. Tirronen, Chem. Eng. Sci. 52 (1997) 3369.
[28] H. Fujimoto, Y. Mizutani, J. Endo, Y. Jinbu, J. Org. Chem. 54 (1989) 2568.
[29] T. Fujita, C. Takayama, M. Nakajima, J. Org. Chem. 38 (1973) 1623.
[30] D. Datta, D. Majumdar, J. Phys. Org. Chem. 4 (1991) 611.
[31] M. Charton, J. Org. Chem. 41 (1976) 2217.
[32] M. Alvaro, A. Corma, D. Das, V. Fornes, H. Garcia, J. Catal. 231 (2005) 48.
[33] A. Corma, H. Garcia, Catal. Today 38 (1997) 257.
[34] F. Omota, A.C. Dimian, A. Bliek, Chem. Eng. Sci. 58 (2003) 3175.
[35] M. Laporta, M. Pegoraro, L. Zanderighi, Phys. Chem. Chem. Phys. 1 (1999) 4619.
[36] R. Buzzoni, S. Bordiga, G. Ricchiardi, G. Spoto, A. Zecchina, J. Phys. Chem. 99 (1995) 11,937.
[37] C.A. Wilkie, J.R. Thomsen, M.L. Mittleman, J. Appl. Polym. Sci. 42 (1991) 901.
[38] R. van Grieken, J.A. Melero, G. Morales, Appl. Catal. A 289 (2005) 143.
[39] A. Baiker, Chem. Rev. 99 (1999) 453.